AD NUMBER: AD0236207

LIMITATION CHANGES

TO:

Approved for public release; distribution is unlimited.

FROM:

Distribution authorized to US Government Agencies and their contractors; Administrative/Operational Use; 5 Apr 1960. Other requests shall be referred to Naval Radiological Defense Laboratory, San Francisco, CA, 94124

AUTHORITY

NRDL ltr dtd 29 Sep 1966

UNCLASSIFIED

Copy No. 105

THE NRDL DYNAMIC MODEL FOR FALLOUT FROM LAND-SURFACE NUCLEAR BURSTS

Research and Development Technical Report USNRDL-TR-410

5 April 1960

by

A. D. Anderson

U.S. NAVAL RADIOLOGICAL DEFENSE LABORATORY
SAN FRANCISCO 24 · CALIFORNIA

UNCLASSIFIED

THE NRDL DYNAMIC MODEL FOR FALLOUT FROM LAND-SURFACE NUCLEAR BURSTS

Research and Development Technical Report USNRDL-TR-410
S-FO11-05-12

5 April 1960

by

A.D. Anderson

Effects of Atomic Weapons

Technical Objective
AW-5c

Weapons Capabilities Branch
C.F. Ksanda, Head

Military Evaluations Division
W.E. Strope, Head

Scientific Director
P.C. Tompkins

Commanding Officer and Director
Captain J. H. McQuilkin, USN

U.S. NAVAL RADIOLOGICAL DEFENSE LABORATORY
San Francisco 24, California

ABSTRACT

A fallout-computation method should be based on all the dynamics of the fallout process, but current computation models do not provide more than generalized answers because they do not account for early-time dynamics. In the attempt to account for the entire process, a theory for close-in fallout was originated. This theory was checked by developing from it a mathematical fallout model for land-surface bursts (the D model) and then using this model to compute fallout dose-rate patterns for two low-yield nuclear tests in Nevada. From a comparison of these patterns with the measured test patterns, it is concluded that the theory, as embodied in the D model, is sound, at least for low-yield land-surface bursts. Also, preliminary results indicate that the theory can be used to give accurate computations for bursts in the moderate and high-yield ranges.

SUMMARY PAGE

The Problem

Currently used fallout-computation methods do not give sufficiently accurate information on close-in fallout for obtaining satisfactory estimates of the radiation doses that personnel would receive; mainly because they are not based on a fundamental theory. In particular, current computation models do not take into account the dynamics of the fallout process before the nuclear cloud reaches its maximum altitude. These models differ more in detail than in principle. They all start the fallout from the nuclear cloud at its maximum altitude. At the time of start of fallout the models all use an estimate of the initial distribution of fallout particles (and hence radioactivity) in space which is based on the height and size of the visible nuclear cloud (and often the stem). A critical examination of the generally-accepted basic assumptions of the various models, such as the time of start of fallout and its initial space distribution, reveals that they are all of doubtful validity. They are convenient, but not necessarily realistic. However, regardless of the assumptions chosen, the models greatly underestimate the very close-in fallout (the fallout in the region surrounding the burst point and extending immediately downwind). Therefore, a new fallout model for close-in fallout is needed.

Findings

In the attempt to explain all the important characteristics of the fallout mechanism, starting with the origin of the nuclear cloud and following through the dynamics to fallout cessation, a theory for close-in fallout is developed. This theory is used as a basis for fallout computation by deriving from it a mathematical fallout model (the Dynamic model or D model) for land-surface nuclear bursts. This model was checked by using it to compute fallout dose-rate patterns for two low-yield nuclear tests in Nevada. From a comparison of these patterns with the measured test patterns, it is concluded that the theory, as embodied in the D model, is sound, at least for low-yield land-surface bursts. Also, preliminary results indicate that the D model can be used to give accurate computations in the moderate and high-yield ranges.

ADMINISTRATIVE INFORMATION

In FY 1960, this project is being sponsored by the U.S. Army under Project Number OD 012-01-001 and by the Navy Bureau of Ships under RDT and E Project Number S-F011-05-12.

ACKNOWLEDGEMENT

Appreciation is expressed to Mr. Endel Laumets, mathematician, for help in deriving the empirical equations expressing nuclear cloud growth.

TABLE OF CONTENTS

LIST OF FIGURES

LIST OF TABLES

1. INTRODUCTION

Currently used fallout-computation methods do not give sufficiently accurate information on close-in fallout for obtaining satisfactory estimates of the radiation doses that personnel would receive; mainly because they are not based on a fundamental theory. In particular, current computation models do not take into account the dynamics of the fallout process before the nuclear cloud reaches its maximum altitude. To attempt to explain all the important characteristics of the fallout mechanism, starting with the origin of the nuclear cloud and following through the dynamics to fallout cessation, a theory for close-in fallout is developed in this paper. This theory is used as a basis for fallout computation by deriving from it a mathematical fallout model for land-surface nuclear bursts.

Close-in fallout-- The term, "close-in fallout," has not been strictly defined and it is likely to remain somewhat arbitrary, since there is nothing inherent in the fallout process itself to provide a distinct boundary between close-in and distant fallout. Operationally, for estimating radiation casualties from fallout, the most satisfactory definition would probably correspond to what is called, "military-significant fallout," and would be based on some limiting dose or dose rate. For example, the region of close-in fallout might be defined as that within which the lifetime

gamma-radiation dose to unprotected personnel exceeds some allowable value, such as 25 roentgens (r). Or it might be defined as that within which the dose rate after fallout cessation exceeds some value, such as 25 r/hr at a standard reference time of 1 hr after burst. Theoretically, since close-in fallout is comprised mainly of particles with significant gravitational falling velocities, it can probably best be defined in terms of a minimum particle size of about 50 microns in diameter. Particles smaller than about 50 microns, exhibit a rapid decrease of falling rate with decrease in size. Consequently, they will remain aloft much longer, be subject to greater dispersion, and settle over much larger areas of the ground than larger particles. Therefore, the dose and dose rate from fallout will tend to fall off rapidly beyond some transition zone, the beginning of which is defined by the arrival of particles of about 50 microns, and beyond which all particles arriving at the ground are less than this size. Since the theoretical size criterion is the more general one, it is better suited to the purposes of this study. Therefore, the following definition for close-in fallout was adopted: Close-in fallout is defined to consist of particles larger than 50 microns in diameter. Accordingly, distant (world-wide) fallout is comprised of smaller particles.

Both the theoretical size criterion and the operational dose (dose-rate) criterion can be applied for any yield. Other criteria which have been used, such as those based on either maximum arrival time at the ground or

maximum distance, hold realistically only for restricted yield ranges, hence they are not as useful. Thus, a definition in terms of fallout down on the ground in 10 hr might be acceptable for high-yield weapons; whereas the appropriate time might be 1 hr or less for low-yield weapons. Distance criteria, such as "fallout within 200 mi," meet the same objection.

Fallout-computation models -- The information desired from the use of a fallout-computation model usually is some measure of the concentration of radioactivity deposited on the ground, or present in some region of space above the ground, as a function of time after burst. From this information, the gamma-radiation dose rate may be computed. The dose rate, or its time integral (dose), has generally been used as a basic parameter in the assessment of radiation hazard. The application of most fallout models has been limited to a computation of the dose rate at a given height above a flat plane (usually 3 ft) resulting from material containing radioactive isotopes deposited on the ground (deposit dose rate). In some circumstances, however, the dose rate from airborne radioactivity during its approach to and passage by a ground location (transit dose rate) may be a significant component of the total dose rate.

There are two stages to most fallout computation models: (1) construction of an initial distribution of radioactive material, involving the assumption of the distribution of radioactivity as a function of position and particle size in the nuclear cloud, and (2) the projection, by graphical or

computational means, of the radioactivity onto its final position on the ground through the influence of the wind structure and gravity.

A variety of models has been developed [Special Committee on Radiation, 85th Congress]. What constitutes close-in fallout for a land-surface burst is defined by the output of these models once all the input variables have been specified, such as the location of the burst point, weapon yield, fission yield, particle-size distribution, size-radioactivity distribution, particle falling rates, cloud geometry, and wind field. These models differ more in detail than in principle. They all start the fallout from the nuclear cloud at its maximum altitude. As far as can be determined, the fallout is started at about the time the nuclear cloud reaches its maximum altitude, which is taken at about 6 min after burst, regardless of yield. At the time of start of fallout the models all use an estimate of the initial distribution of fallout particles (and hence radioactivity) in space which is based on the height and size of the visible nuclear cloud (and often the stem)—radically different assumptions have been made in the various models as to this initial distribution. A critical examination of all the generally-accepted basic assumptions used by the various models, such as time of start of fallout and its initial space distribution, reveals that they are all of doubtful validity. They are convenient, but not necessarily realistic. For example, the assumption that

the radioactive fallout cloud is totally contained within the visible cloud (and stem) when the latter reach maximum altitude is not borne out by experimental facts. In other words, there is no definite proof that the fallout space distribution has any obvious relation to the visible cloud boundaries. Three other conditions are commonly assumed to hold when the visible cloud reaches its maximum altitude. These are; (1) that the fraction of the total radioactivity at any relative altitude in the cloud is independent of the yield, (2) that the percentage particle-size distribution is the same throughout the cloud, and (3) that this size distribution is independent of the yield. Actually, the results of this study demonstrate that the radioactivity and size distributions at any altitude in the cloud vary markedly with yield and time. However, regardless of the assumptions chosen by the models, they greatly underestimate the very close-in fallout (the fallout in the region surrounding the burst point and extending immediately downwind).

These are some of the reasons why present models are considered grossly inadequate. The basic reason for the drawbacks of current models has been obvious for some time--they are inaccurate because they are not based on a fundamental knowledge of the fallout mechanism. In view of this, before the endeavor was made by the author to develop a reliable model for land-surface bursts, a theory for close-in fallout was

attempted first. This theory is presented in the next section.

2. A THEORY FOR CLOSE-IN FALLOUT

In order that the basis for the formulation of the theory for close-in fallout may be better understood, a description of a land-surface nuclear burst is given. Particular emphasis is placed on the interval from the time of formation of the visible cloud to the time this cloud reaches its maximum altitude. To provide the key to comprehending the pertinent dynamics, the formation and nature of fallout particles are discussed also.

The land-surface nuclear burst-- The land-surface burst is defined as one in which the fireball touches the ground. Ordinarily, its burst height above the ground can vary considerably, and it will still produce appreciable fallout. However, in the following discussion, a contact surface burst will be implied whenever a land-surface burst is mentioned. It is considered the most important type of burst for which fallout computation is required, since in this case many heavy soil particles come in contact with the radioactive fission products (a mixture of weapon materials and radioactive isotopes) in the fireball and create hazardous close-in fallout. In the case of an air burst (one in which the fireball does not touch the ground) no heavy soil particles become contaminated with fission products, hence such bursts will produce much less severe close-in fallout conditions.

Following is a description of a land-surface burst: Immediately after

detonation, all of the weapon materials--including radioactive isotopes--exist in the form of vapor in the fireball. The fireball grows rapidly in size and within several seconds after burst starts to move upward rapidly. The center of the fireball moves upward more rapidly, generating a vortex ring (toroid). Immediately after the fireball begins to rise, air--carrying surface material--rushes into its bottom, forming the dust-laden stem. As the fireball cools, the materials within it (including water vapor) condense or solidify, and the familiar rising mushroom cloud is formed. The cloud stops rising after several minutes shortly after its internal temperature has become approximately equal to ambient. Since the cloud is extremely turbulent initially, particles taken into the cloud should be thoroughly mixed throughout its volume, together with the radioactive fission products. However, as the cloud ascends, its rate of rise decreases; hence, more and more of the larger radioactive particles fall out, and the result is an altitude distribution of particle sizes that becomes more marked the higher the cloud rises from the ground.

Formation of radioactive particles--Various mechanisms have been suggested to account for the details of the formation of fallout particles from a land-surface burst. The most likely explanation is that the origin of the radioactive fallout particles lies in the interaction of the condensing

vaporized materials, containing radioactive isotopes, with the entrained and heated earth materials in the fireball [Adams et al]. The process of condensation alone produces particles too small to descend in appreciable quantities. In other words, particles which enter the fireball before the temperature has been sufficiently reduced are vaporized and do not participate in close-in fallout. Particles of sufficient size to fall in a relatively short time are formed only when the vaporized material combines with the earth material, either by direct condensation onto the earth material or by first condensing into small particles and then impacting on and adhering to the earth material. Since observations of fallout particles from tests in Nevada and the Pacific show that in all except a few cases the radioactivity is associated with earth material that had been fused, but not vaporized, the time at which the fireball temperature drops and remains below the vaporization temperature of the earth material can be regarded as the beginning of the time of formation of the radioactive fallout particles. Likewise, the time at which the fireball temperature drops and remains below the melting point of the earth material can be regarded as the end of the time of formation of the radioactive particles. These times, which are yield dependent, can be estimated from the temperature-time relation for the fireball (as will be shown later).

Inasmuch as the earth material usually consists of a mixture of

substances, it cannot be said to have a fixed vaporization or melting point. However, it is possible to make useful estimates nevertheless. For example, for Nevada soil, the most refractory of the silicate minerals, quartz, boils at 2230°C; the mineral having the minimum melting point, about 1100°C, is feldspar. Consequently, each of the major components of the original soil would be in the form of liquid droplets sometime during the period when the fireball temperature is between 2230°C and 1100°C. Therefore, the time at which the fireball temperature drops and remains below 2230°C can be regarded as the beginning of the time of formation of the Nevada radioactive fallout particles, and the time at which the temperature drops and remains below 1100°C can be regarded as the end of the time of formation of the particles.

Time of the start of fallout -- The time at which the fireball's temperature has dropped below 2230°C (after its second temperature maximum) can be taken, for most purposes to be the time of start of fallout for Nevada-type (siliceous) soils. This can be done because the start time is not very sensitive to the fireball temperature, since it falls off very rapidly after its second maximum. Also, for this same reason, the time of start of fallout should be relatively insensitive to soil type (soil vaporization temperature).

To derive the time of the start of fallout for Nevada-type soil,

t_o, in seconds after burst, the following equation [U.S. Atomic Energy Commission] is used:

$$t_o/t_m = K \quad , \tag{1}$$

where t_m is the time of the fireball's second temperature maximum, equal to $0.032\ W^{1/2}$ (where W is the yield in kilotons), and K is a constant having the same value for a given t_o for all yields. Since the temperature of the whole fireball is fairly uniform after its second maximum, the value of K can be estimated for $t_o = 2230^{\circ}C$ from Figure 2.92 of the U.S. Atomic Energy Commission [1957], which gives the variation of surface temperature with time for a 20-kiloton burst. (The type of burst is not stated, however an analysis of limited test data indicates that the temperature-time curves for a surface and an air burst, both of the same yield, will not be significantly different after the second maximum.) From Figure 2.92, $t_o = 2.1$ sec and $t_m = 0.15$ sec; hence, from Equation 1, $K = 2.1/0.15 = 14.0$. Consequently, for any yield, W,

$$t_o = 14.0 \times 0.032\ W^{1/2} = 0.45\ W^{1/2} \quad . \tag{2}$$

Equation 2 shows that the time of the start of fallout varies directly as the square root of the yield, and is about 0.4 sec for 1 kiloton (kt), 4.5 sec for 100 kt, and 45.0 sec for 10 megatons (mt). The time of the

end of the formation of the radioactive fallout particles, t_e, the time in seconds after burst it takes for the fireball temperature to drop to 1100°C, can be derived in a similar fashion. Here, K = 20.0, consequently, $t_e = 10\ t_o/7$. Therefore, the time of the end of formation varies from about 0.6 sec for 1 kt, 6.4 sec for 100 kt, and to 64.3 sec for 10 mt. Hence, the time interval during which fallout is created varies from about 0.2 sec for 1 kt, 1.9 sec for 100 kt, and to 19.3 sec for 10 mt.

It was mentioned that all fallout models start the fallout from the cloud (and sometimes the stem) when it reaches its maximum altitude, which is taken usually at about 6 min after burst, regardless of yield. However, since Equation 2 shows that the time of the start of fallout is less than 45 sec after burst for yields less than 10 mt, a satisfactory physical explanation for very close-in fallout (which was underestimated by all models) is that it results from the fallout of the heavier particles from the visible cloud into the air surrounding the stem during the time the cloud is still rising to its maximum altitude (actually, the stem occupies only a small portion of the cross-section area under the cloud). Hence, it is likely that the fallout near and surrounding the burst point (ground zero) does not come from the stem; it comes from the base of the visible cloud as it rises. Therefore, Equation 2 definitely indicates that the computation of fallout particle trajectories should be commenced not at the time the

visible cloud reaches maximum altitude but much earlier, near the time when the visible cloud first forms and begins to rise. Thus, one of the premises basic to the theory is that the radioactive fallout is created and fallout starts within a relatively short time after detonation, much before the visible cloud reaches its maximum altitude.

Motion of fallout particles-- Basically, the problem of computing fallout resolves itself into following the motion through the atmosphere of a large group of fallout particles from the time of their formation, shortly after detonation, until their subsequent deposition over the countryside. What is required is a knowledge of the initial position of each fallout particle and a time history of its upward, downward, and horizontal movement. Establishing when, where, and how the actual fallout is assumed to start is of particular importance in determining the particle trajectories. The theory for close-in fallout attempts to take into account the motion of the radioactive fallout particles from the time of their inception in the initial visible cloud until they finally return to the ground. The theory does this by considering the effect of the rise of the visible cloud on a particle's rise and fall and the effect of the winds in displacing the particle horizontally. The resultant motion is the particle trajectory. The theory assumes that all the radioactivity deposited on the ground, even that in the vicinity of the crater, results from the fall of

individual particles originating from the initial visible cloud. Hence, the fireball which has risen from the ground, and consequently, the initial visible cloud, contains all the residual radioactivity.

At the time of the start of fallout it is assumed that the radioactive particles created are uniformly mixed throughout the initial visible cloud by the extreme turbulence. Therefore, at this time the initial radioactive-particle cloud is taken to have a uniform distribution of particle sizes contained in a volume coincident with that of the newly-formed visible cloud. After fallout has started, the motion of these particles consists of two independent components, vertical and horizontal, both of which are functions of time and space. The vertical (upward and downward) motion of the particles is obviously governed by the rising motion of the cloud and gravity. Thus, the rate with respect to the ground at which a particle moves upward or downward is taken equal to the difference between the velocity with which it is carried up by the rising cloud and the velocity with which it falls (due to gravity). This assumption of net particle-falling rate forms another of the basic premises of the theory. Vertical winds may affect the rising and falling rate, but, in most cases, they have not been considered important in predicting close-in fallout. Also, during the formation of the visible cloud, the toroidal circulation that is induced persists usually until after the cloud

has stopped rising. Although there is little known about the effect of this circulation on the particles, it is presumed that its net effect on the gravitational settling of the particles is negligible. That is, it is presumed that the circulation does not displace the mean center of gravity of the fallout-particle mass.

Consequently, at any time after the start of fallout a particle's velocity with respect to the ground, $\dot{z}$, can be taken as:

$$\dot{z} = U - V \quad , \tag{3}$$

where U is the particle's upward velocity due to the rise of the cloud, and V is its downward velocity due to gravity. Here $\dot{z}$ is taken to be positive when the particle is moving upward, that is, $(U - V) > 0$. The particle is moving downward when $(U - V) < 0$. Large particles reach their maximum altitude and start falling while smaller particles are still rising. The altitude of the particle, z, at any time t before it reaches the ground is found by integrating the particle's velocity over time:

$$z = \int_{t_o}^{t} (U - V)\, dt + z_o \quad , \tag{4}$$

where t_o is the time of the start of fallout (Equation 2 for Nevada-type soil) and z_o is the altitude of the particle at this time (the initial altitude).

Horizontal motions of the fallout particles have generally been

considered to result from the existing winds, although atmospheric turbulence may produce a certain amount of dispersion. But, in most cases, this dispersion is small compared to the spread of the particles produced by wind shear and is ignored in computing close-in fallout. Additional horizontal motions are caused by the expansion of the cloud; this effect is taken into account later (Equation 18). Only the horizontal component of motion due to the horizontal winds will be examined now.

Wind speed and direction at the various altitudes are two of the most important factors which determine the distribution of fallout on the ground. As a particle rises and then falls, it is carried horizontally by the wind. The time during which it is rising (falling) through a given altitude range or layer is inversely proportional to its rate of rise (fall). Thus, its maximum horizontal travel during its entire rise (U>V) from its initial altitude, z_o, to its maximum altitude, z_m, and during its entire fall (V>U) from z_m to the ground, at elevation z_g, can be expressed as the total of two summations of its horizontal travel in each layer:

$$\underset{\sim}{H} = \sum_{z_o}^{z=z_m} \frac{\underset{\sim}{W}(z)\Delta z}{U - V} + \sum_{z_m}^{z=z_g} \frac{\underset{\sim}{W}(z)\Delta z}{V - U} \qquad (5)$$

where $\underset{\sim}{H}$, a vector, is the maximum horizontal displacement of the particle from ground zero; $\underset{\sim}{W}$, a vector, is the wind velocity (a function of z);

Δz is the altitude-layer thickness; and U and V are defined for Equation 3.

Complete particle trajectories can be found for any particular detonation by combining the vertical and horizontal components of motion. The particle-trajectory data joined with particle-size weighting factors for radioactivity make possible quantitative computations of the radioactivity present at any point for a given time, either on the ground or at a specified altitude. Of course, it is not practicable to follow the trajectory of each individual particle. In the computations the particles are dealt with by size classes, as will be demonstrated later.

Results from the theory-- The theory is illustrated by Anderson [1958] for JANGLE-Surface, a 1.2-kt contact land-surface burst, by deriving certain properties of the fallout from the computation of the vertical motions alone. These properties occur irrespective of the existing winds and lateral fallout dimensions. There is a marked advantage in using such an approach because major uncertainties often exist in the winds and the cloud geometry data. In particular, the following properties of the fallout process were considered: (1) times of fallout arrival and cessation at the ground for particles of given sizes; (2) size distribution of fallout particles at the ground at a given time; and (3) altitudes of given size particles at a given time. The fallout properties enumerated above are essentially dynamic ones, and the correctness of a model can be best

ascertained by checking its ability to predict these properties. However, it has been the practice to check models by comparing the model-derived fallout patterns (dose-rate contours of the deposited fallout) for the various weapons tests with those derived from measurements made at many locations. Hence, this method will be adopted (later in this paper) for checking the theory.

3. THE DYNAMIC FALLOUT MODEL

To check the validity of the new theory as a basis for computing fallout from land-surface bursts, a mathematical model is developed from the theory. This model, called the Dynamic or D model, is programed for the U.S. Naval Radiological Defense Laboratory (USNRDL) computer which is used to compute fallout dose-rate patterns for the following two low-yield nuclear tests conducted at the Nevada Test Site: JANGLE-Surface, a contact surface burst, and JANGLE-Underground, a shallow underground burst. These patterns are then compared with patterns constructed from data measured at the tests (Section 4).

General description-- The Dynamic model represents the particle-size distribution (and hence distribution of radioactivity) of fallout in space and time by means of the trajectories of a number of circular disks, each denoting a given particle-size class. The fallout dose-rate pattern on the ground is derived by combining the particle-trajectory data with

particle-size weighting factors for radioactivity and applying knowledge of the fallout-radiation-energy spectra and attenuating characteristics of the air and ground surface.

The trajectory of the center of each disk is found from the particle-size time-altitude history and the wind velocity data. The model takes into account the drift of the particles due to the wind acting on them during their rise to their respective maximum altitudes (Equation 5), an important effect usually neglected in other models. This is necessary not only for computing close-in fallout, and especially very close-in fallout, but also for calculating such other factors as the transit dose rate. The centers of the disks are tracked, first upward and then downward, to the ground. Since each disk contains a certain percentage of the total residual radioactivity, the total dose rate contributed by the disks to a selected ground location at any time after burst can be deduced by noting the time of arrival of those centers falling within one disk radius of that location. This can be done fairly accurately provided that once the fallout lands on the ground it is not significantly disturbed by the surface winds.

Initial conditions-- At the time of start of fallout (Equation 2) the initial radioactive particle cloud containing the total residual radioactivity is assumed to have a uniform distribution of particle sizes contained in a

volume coincident with that of the newly-formed visible cloud. This initial particle cloud (whose top, base, and diameter are given by Equations 7, 8, and 18, respectively) is depicted by 68 identical coincident right-circular cylinders, each of which represents a selected particle-size class ranging from 40-60 microns up to 8700-10,000 microns in diameter (Table 1). This follows the assumption mentioned previously that each particle size comprising the fallout is dispersed uniformly throughout the initial visible cloud. Each cylinder is divided up into N equisize disks (N varies from 7 for 0.01 kt to 231 for 100 mt, hence the total number of disks used varies from 476 for 0.01 kt to 15,708 for 100 mt); therefore, each disk represents a portion of a selected particle-size class. In order to calculate the motion of a given disk (size-class portion), the particle size at the midpoint of the size class (Table 1) is used. A particle of this size is assumed to be at the center of the disk; for this reason, a trajectory for this particle denotes a trajectory for the center of the disk. The method of finding the fraction of the total activity in each size range shown in the table will be discussed later in this section.

Time-altitude history of particles -- The integral in Equation 4 is approximated by a finite difference equation by dividing the time interval from the time of the start of fallout, t_o, to the time a particle reaches the ground, t_n, into n smaller intervals, Δt_o, Δt_1, ..., Δt_{n-1}, starting

Table 1--D-model fallout-particle size ranges and radioactivity

Size range (microns)	Midpoint size (microns)	Fraction of total activity in range	Size range (microns)	Midpoint size (microns)	Fraction of total activity in range
40-60	50	0.0841	380-400	390	0.0092
60-80	70	0.0648	400-420	410	0.0086
80-100	90	0.0520	420-440	430	0.0080
100-120	110	0.0429	440-460	450	0.0075
120-140	130	0.0362	460-480	470	0.0070
140-160	150	0.0310	480-500	490	0.0066
160-180	170	0.0270	500-520	510	0.0062
180-200	190	0.0237	520-540	530	0.0058
200-220	210	0.0210	540-560	550	0.0055
220-240	230	0.0188	560-580	570	0.0052
240-260	250	0.0169	580-600	590	0.0050
260-280	270	0.0153	600-650	625	0.0113
280-300	290	0.0139	650-700	675	0.0100
300-320	310	0.0127	700-750	725	0.0089
320-340	330	0.0117	750-800	775	0.0080
340-360	350	0.0108	800-850	825	0.0072
360-380	370	0.0100	850-900	875	0.0065

Table 1--D-model fallout-particle size ranges and radioactivity (Continued)

Size range (microns)	Midpoint size (microns)	Fraction of total activity in range
900-950	925	0.0059
950-1000	975	0.0054
1000-1100	1050	0.0094
1100-1200	1150	0.0080
1200-1300	1250	0.0068
1300-1400	1350	0.0059
1400-1500	1450	0.0052
1500-1600	1550	0.0046
1600-1700	1650	0.0040
1700-1800	1750	0.0036
1800-1900	1850	0.0032
1900-2000	1950	0.0029
2000-2100	2050	0.0026
2100-2200	2150	0.0024
2200-2300	2250	0.0022
2300-2400	2350	0.0020
2400-2500	2450	0.0018
2500-2600	2550	0.0017
2600-2700	2650	0.0016
2700-2800	2750	0.0014
2800-2900	2850	0.0013
2900-3000	2950	0.0012
3000-3300	3150	0.0032
3300-3600	3450	0.0026
3600-3900	3750	0.0022
3900-4200	4050	0.0018
4200-4500	4350	0.0016
4500-4800	4650	0.0013
4800-5100	4950	0.0012
5100-6000	5550	0.0027
6000-6900	6450	0.0019
6900-7800	7350	0.0014
7800-8700	8250	0.0010
8700-10,000	9350	0.0011

with a 1-sec interval ($\Delta t_o = t_1 - t_o = 1$ sec) and with each succeeding interval becoming progressively larger, increasing by 1, 2, or 3 sec, until the cloud reaches maximum altitude (this allows for the greater changes taking place initially in the rates of rise of the cloud). Thus, Equation 4 is approximated by

$$z = \sum_{i=0}^{n-1} (\bar{U}_i - \bar{V}_i) \Delta t_i + z_o \quad , \tag{6}$$

where i = 0, 1, 2, ... n-1, and $\bar{U}_i$ and $\bar{V}_i$ are mean values for the upward and downward velocities, respectively, (Equation 3) for the time intervals indicated by the subscripts. In Equation 6, $\bar{U}_i$ becomes zero after the visible cloud reaches its maximum altitude (Equation 9).

Rate of rise of visible cloud-- The mean values, $\bar{U}_i$, representing the rise of the cloud can be derived from knowledge of the time-altitude history of the cloud top and base. To do this, empirical expressions giving the altitudes of the cloud top and base as a function of yield and time are used. These equations, which were deduced from nuclear cloud data, are as follows:

$$z_T = 750\ W^{1/4} t^{1/2} \quad , \tag{7}$$

and

$$z_B = 340\ W^{1/4} t^{1/2} \quad , \tag{8}$$

where z_T and z_B are respectively the altitudes of the cloud top and base in feet above mean sea level, W is the yield in kilotons, and t is the time

in seconds after burst. These equations hold fairly well for yields from about 0.01 kt to 20,000 kt for typical atmospheric conditions in the middle and tropical latitudes. They are valid from the time of the start of fallout (Equation 2) up to the time the cloud reaches maximum altitude (the top and base of the cloud both reach maximum altitude at approximately the same time). This time is about 6 min after burst for yields from 0.01 kt to 100 kt, regardless of yield. The time in seconds after burst to reach maximum altitude, t_M, for yields greater than 100 kt is,

$$t_M = 510.3 - 33.9 \ln W, \tag{9}$$

where W is the yield in kilotons. This equation shows that the higher the yield above 100 kt, the shorter the time for the cloud to reach maximum altitude. For example, the cloud from a 20 mt burst will take only 180 sec to reach its maximum altitude. Heretofore, it has been widely believed that all nuclear clouds reach their maximum altitudes at about the same time, at about 6 min after detonation, regardless of yield [Eighty-fifth Congress, p. 281].

The maximum altitude of the cloud, z_M, as a function of yield for yields greater than 100 kt can be found by substituting t_M for t in Equation 7, thus,

$$z_M = 750\, W^{1/4}\, t_M^{1/2} \quad . \tag{10}$$

In using Equations 7, 8, 9, and 10, it must be recognized that the calculated values will differ somewhat from those existing in the real atmosphere due to variations in conditions (particularly the atmospheric stability and moisture content). However, normal variations will not introduce significant errors in the D-model computations.

Generally, from Equations 7 and 8, the altitude of any particular small parcel of the cloud, z_C, is

$$z_C = k\, W^{1/4} t^{1/2} \quad , \tag{11}$$

where $z_B \leq z_C \leq z_T$, and k is a constant depending on the parcel's relative altitude in the cloud, which remains unchanged, so that $340 \leq k \leq 750$. Therefore, if Δz_C is the change in the cloud parcel's altitude during the finite time interval $\Delta t_i = t_{i+1} - t_i$, then

$$\bar{U}_i = \frac{\Delta z_C}{\Delta t_i} = \frac{k\, W^{1/4} t_{i+1}^{1/2} - k\, W^{1/4} t_i^{1/2}}{t_{i+1} - t_i} = \frac{k\, W^{1/4}}{t_i^{1/2} + t_{i+1}^{1/2}} \quad . \tag{12}$$

In order to use Equation 6 to compute fallout particle time-altitude histories, it is convenient to transform Equation 12 by substituting for k the expression $z_C / W^{1/4} t^{1/2}$ (from Equation 11), giving

$$\bar{U}_i = \frac{z}{t_i^{1/2} \left(t_i^{1/2} + t_{i+1}^{1/2} \right)} \quad , \tag{13}$$

where z (substituted for z_C) is the altitude of the particle at time t_i (substituted for t). Equation 13 reveals that $\bar{U}_i$, for any given time interval, decreases linearly with decreasing altitude in the cloud. In the D-model computations it is assumed that the same rate of decrease applies in that region beneath the cloud which extends from the cloud base to the ground. This ignores the much higher velocities in the stem. However, since the stem occupies only a relatively small portion of the region beneath the cloud, its effect is not significant. Probably the main objection to this assumption is the fact that the upward air motion below the cloud has an inwardly-directed horizontal component as well as a vertically-directed upward component. This motion would tend to move the heavy particles, falling out of the cloud first, in toward the burst point. However, this appears to be of consequence only in predicting fallout very close to ground zero.

Terminal velocity of particles-- The $\bar{V}_i$ terms in Equation 6 are the average downward terminal velocities in still air of the particles during the time intervals indicated by the subscripts. A convenient equation for computing the terminal velocities of the irregular particles used in the D model has been derived by Ksanda of NRDL [private communication]. This equation, which takes into account both inertial and viscous forces, is:

$$y = 1.325 \log_{10}^{3} (x + 1.163) \quad , \tag{14}$$

$$\text{where } y = V\left[\frac{\rho_o^2}{2\eta(\rho - \rho_o)}\right]^{1/3}, \text{ and}$$

$$x = d\left[\frac{2g\rho_o(\rho - \rho_o)}{\eta^2}\right]^{1/3}.$$

Here, V is the particle terminal velocity, ρ, the particle density (which for Nevada-type soil is taken as 2.6 g/cu cm), ρ_o, the air density, g, the acceleration due to gravity, η, the air viscosity, and d, the particle diameter. The accuracy of Equation 14 is doubtful for particle diameters of less than 20 microns. For particles at high altitudes, where the air density is very low, V is multiplied by $1 + \frac{L}{d}\left[2.514 + 0.800 \exp\left(-0.55\frac{d}{L}\right)\right]$ [Davies], where L is the mean free path of the air molecules. In the D model, the ρ_o and η values used are normally those selected from the ARDC Model Atmosphere [Minzner et al], which is essentially a mid-latitude standard atmosphere. For most types of calculations performed with the D model the values from this atmosphere can be used without introducing significant error. However, such values apply only for the ambient atmosphere, whereas the values for the actual conditions inside the cloud may be quite different. However, for yields less than about 1 mt the latter values rapidly approach ambient after the start of fallout; hence, the terminal velocities computed for the ambient atmosphere for these yields are not significantly different from those inside the cloud.

Ground distribution of particles--In order to find a particle's ground impact point Equation 5 is rewritten as follows:

$$\underset{\sim}{H} = \sum_{i=0}^{n-1} \underset{\sim}{\bar{W}}_i \Delta t_i \quad , \tag{15}$$

where $\underset{\sim}{\bar{W}}_i$ is the mean wind velocity (average wind speed and direction) in the layer Δz_i traversed by the particle during the time interval Δt_i (the Δt_i values are the same as those used in Equation 6). The base and top of Δz_i is found from Equation 6, and $\underset{\sim}{\bar{W}}_i$ is determined from wind velocity-altitude data. Consequently, the ground impact point (the maximum horizontal displacement of the particle from ground zero) is found by adding together vectorially all the individual displacements undergone by the particle while in the air. Using this method, not only can the fallout particle ground distribution (and hence radioactivity) be determined but also changes in the configuration of the radioactive fallout cloud with time and space can be represented fairly effectively.

Fallout particle radioactivity-- The fraction, F, of the total residual radioactivity associated with each particle-size class (Table 1) was found from the following equation:

$$F = \frac{1}{\sigma \sqrt{2\pi}} \int_{\phi_1}^{\phi_2} \exp \left[\frac{-(\phi - \bar{\phi})^2}{2\sigma^2} \right] d\phi \quad , \tag{16}$$

where for the size class μ_1 to μ_2, $\phi_1 = \log \mu_1$, $\phi_2 = \log \mu_2$, $\phi = \log \mu$, $\bar{\phi} = \overline{\log \mu} = 2.053$ (the average value of $\log \mu$), and $\sigma = 0.732$. This equation was derived from Figure 1, which shows for each particle diameter (in microns) plotted vertically on a logarithmic scale, the percentage of activity associated with all particles greater than that size plotted horizontally on a probit scale. The straight-line plot means that the radioactivity has a normal distribution with respect to the logarithm of the particle diameter. The data points in Figure 1, derived from measurements made at JANGLE-Underground [Anderson, 1959, p. 10], is for Nevada soil which possesses properties similar to soils commonly found throughout the world. How well the data of Figure 1 hold for surface bursts occurring over different soils and varying over a wide range of yields is unknown. For most siliceous soils, the sparse data available indicate that for close-in fallout the fraction of radioactivity in a given size range is roughly constant regardless of yield. However, the size-radioactivity distribution for coral is markedly different from that for siliceous soil. For surface bursts in the Pacific, in which the soil consists mostly of coral, an analysis of Operation REDWING data by Ksanda of NRDL [private communication] indicates that the size-radioactivity distribution can be represented by Equation 16, with $\bar{\phi} = 2.209$ and $\sigma = 0.424$.

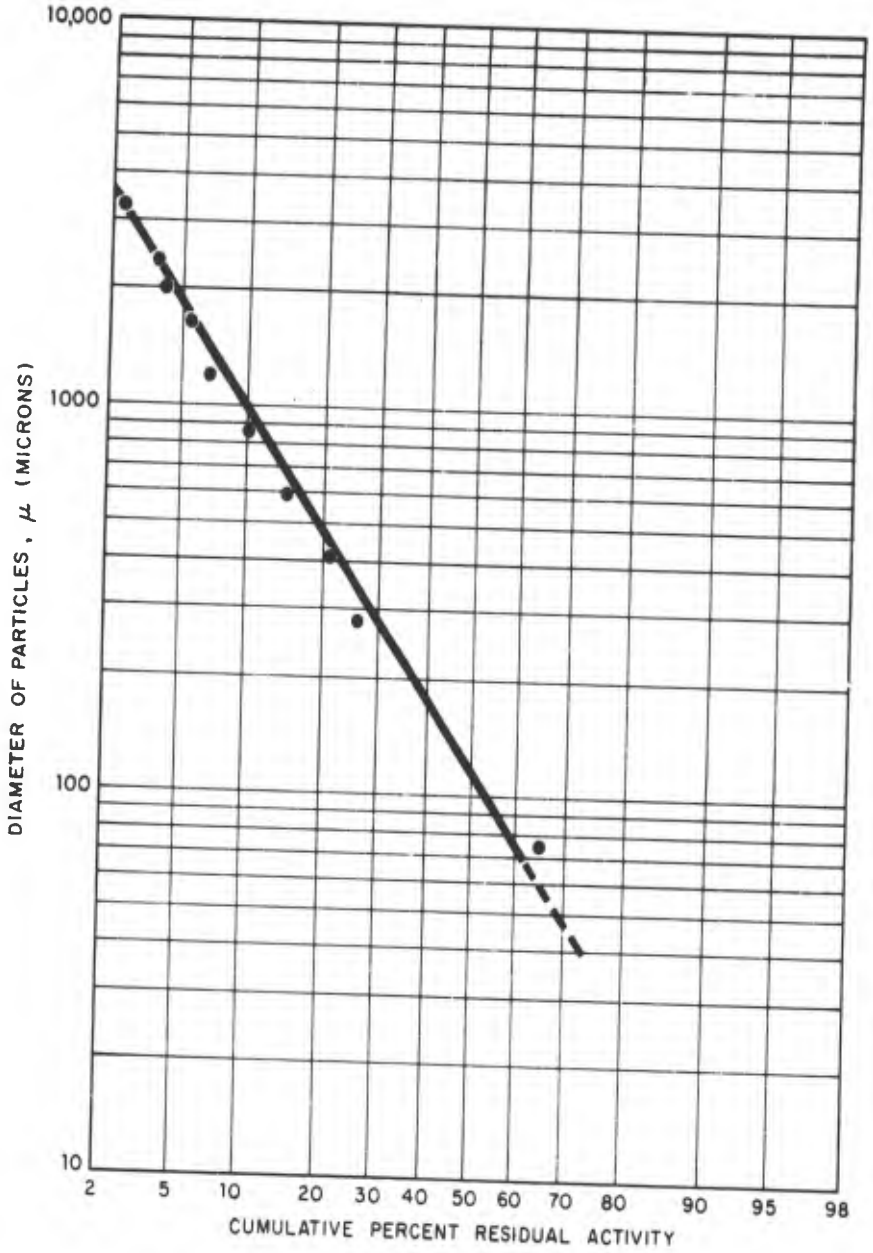

Fig. 1 Cumulative Percent of Residual Activity in All Particles $> \mu$ for J-U

If N is the number of disks used to represent the size class from μ_1 to μ_2, then the fraction of the total residual radioactivity in each of these disks is F/N.

Calculation of deposit dose rate--If one of the disks representing the μ_1 to μ_2 size class lands on the ground before 1 hr after burst and covers a point P on a rough plane, then the deposit dose rate, R, in r/hr at 1 hr and 3 ft above this location is expressed by Ksanda [Anderson, 1959, p. 44] as:

$$R = 120\ F\ A/NS \quad , \tag{17}$$

where 120 is a constant that among other things takes minor surface irregularities into account, F is defined by Equation 16, A is the total residual radioactivity in curies remaining at 1 hr after burst, and S is the area in square feet on the ground covered by the radioactivity contained in the disk. The edge effect is ignored. That is, if the disk covers the point P when it reaches the ground, then its contribution to the dose rate at 3 ft above P is approximated by assuming the disk is an infinite rough plane. If the disk fails to cover P, the contribution is zero. The edge effect is not important except for regions immediately adjacent to intense gradients of radioactivity. The total deposit dose rate at P is the sum of the individual dose rates contributed by the disks that cover this location. Since the effects from induced activities and

fractionation are not well known, they are not taken into account. Their significance for close-in fallout computation has not yet been determined. Experience with the D model thus far does not indicate that they are important in most situations.

In Equation 17, A is determined from the known total fission product radioactivity released at burst for each kiloton of yield, about 1.5×10^{23} fissions/kt [Government of India] by calculating the effects of radioactive decay using the data by Glendenin appearing in Bolles and Ballou [1956]. These decay data are presented in the form of the activities in disintegrations per second (dis/sec) of the total fission product mixture at various times after the slow neutron fission of 10,000 atoms of U^{235}. Since, by definition, one curie = 3.7×10^{10} dis/sec, it is found by calculation that each kiloton of yield gives 5.0×10^{8} curies of radioactivity at 1 hr after burst. Hence, $A = 5.0 \times 10^{8}$ W, where W is the yield in kilotons. This value of A applies for a fission yield of 100 per cent; however, if the fission yield is less, A can be adjusted by simple proportionation. In determining S, it is assumed that the distribution of the equisize particles (radioactivity) in each disk is uniform (each disk is uniformly contaminated). In any case, experience has indicated that the fallout dose-rate pattern is not sensitive to the radial distribution except near its periphery. Since the disks are circular,

S is taken equal to πr^2, where r is the radius of the disk. The method of finding the radius of each disk is based on the following three assumptions: (1) the fallout (every particle size) is dispersed uniformly throughout the initial visible cloud at the time of start of fallout, (2) as the cloud expands, the fallout (every disk) expands laterally at the same rate as the cloud, and (3) the lateral expansion of the fallout stops after the cloud has stopped expanding. With regard to assumptions 1 and 2, there is some evidence that at short times after burst, before the visible cloud reaches maximum altitude, the diameter of the radioactive cloud is smaller than that of the visible cloud, especially for the higher yields. Nevertheless, in the absence of more specific information, the D model does not attempt to take this effect into account. Regarding assumption 3, the disk diameters can be held constant after the cloud has stopped expanding since for the time intervals considered for computing close-in fallout the spread of the falling particles due to small-scale turbulence and diffusion can normally be ignored.

An analysis of nuclear cloud data yielded the following empirical expression for the horizontal diameter of the visible cloud as a function of yield and time:

$$D = 1085\, t^{0.25}\, W^{0.11}\, t^{0.22} \quad , \tag{18}$$

where D is the horizontal diameter in feet, t is the time in seconds after burst, and W is the yield in kilotons. This equation holds fairly well for yields from 1 kt to 20,000 kt (for yields less than 1 kt, the factor $t^{0.22}$ is dropped from the second exponent). It is valid from the time fallout starts to the time the cloud stops expanding; for yields up to about 100 kt the latter occurs at the time the cloud has reached its maximum altitude (6 min). For higher yields the visible cloud continues to expand laterally for an undetermined time, about 1-10 min, after reaching maximum altitude. Evidently, this effect is due to the toroidal circulation, which grows in diameter as the cloud decelerates.

Since the larger particles will fall out of the visible cloud before it reaches its maximum diameter, the diameter of each of the disks representing these particles is taken equal to the horizontal diameter of the expanding visible cloud at the timme each disk leaves the base of the cloud (using Equations 6, 8, and 18). This assumes, of course, that the disks change their diameters only while they are under the influence of the expanding visible cloud. In the D model, a maximum disk diameter for all yields is taken as that given for t = 360 sec (6 min) in Equation 18. Using this "cut-off" diameter does not commonly result in meaningful error being introduced in the computations. It may be noted that other fallout models generally use only one disk diameter, usually that

corresponding to some estimated maximum cloud diameter. However, it is especially important to use variable diameters for the disks used to represent the very close-in deposit fallout in the region surrounding the burst point. It is also necessary to use variable-disk diameters for fractional-kiloton bursts--it has been found that almost all of the close-in deposit fallout from very low yield bursts consists of particles which have fallen out of the base of the nuclear cloud before it reached maximum altitude.

Calculation of deposit dose-- If the dose-rate history (dose rate vs time) is known for a location P, then the deposit dose can be calculated for any time interval. This means that the time at which the disks arrive at P must be taken into account. For example, the deposit dose in roentgens received from a given disk during a specified interval from t_a to t_b hours after burst is,

$$\text{Deposit dose} = R \int_{t_a}^{t_b} t^{-\lambda}\, dt = \frac{R}{1-\lambda} \left(t_b^{1-\lambda} - t_a^{1-\lambda}\right) \quad , \qquad (19)$$

where R is defined by Equation 17, and λ is the decay constant for the fallout gamma radioactivity (λ varies with time after burst but can be held constant for short time intervals, $t_a - t_b$). The total deposit dose received at P during the interval t_a to t_b then is the sum of the individual doses from the disks that arrive at P before and during the time interval.

Computer program for D model-- The D model is programed for the NRDL electronic computer (Datatron 205, a medium-speed computer). Computations are being made in great detail for fallout deposit dose-rate and dose patterns for land-surface bursts for yields from 0.01 kt to 100 mt (Program 3020). The only input data necessary are the yield (total and fission) and winds. Since the D model gives the location in space of all the radioactive particles at any time, the dose rate or dose from the airborne material can be computed. Thus, a program has been developed (Program 3033) to compute the transit fallout effects. Because of the complexity of the D model, computations for a given yield and wind condition take many hours to make. Deposit-fallout calculations range from about 6 hr for 0.01 kt to 100 hr for 10 mt; transit-fallout calculations take much longer.

4. COMPARISONS BETWEEN COMPUTED AND OBSERVED FALLOUT PATTERNS

In this section the theory's ability to reproduce the actual fallout process is estimated by comparing the dose-rate fallout patterns computed by the D model with the observed test patterns (patterns constructed from measurements) for JANGLE-Surface (J-S), a surface burst, and JANGLE-Underground (J-U), a shallow underground burst, detonated at 17 ft beneath the surface. These Nevada shots are selected because they represent the land-surface type of burst and were of the same yield, namely, 1.2 kt.

The first emphasis has been placed on low yields because more adequate test data are available for them and because fallout computation is much less time consuming for low yields than for high yields. However, the basic fallout phenomena associated with a high yield are essentially the same as those for a low yield, at least for surface and shallow-underground bursts. Any differences that may exist are probably ones of degree rather than of kind.

Only a gross comparison is possible for estimating how well the theory, as embodied in the D model, describes the fallout process. Unfortunately, there is no acceptable method for objectively judging the validity of a fallout theory or model, mainly because of the lack of knowledge of the various fallout phenomena, the interactions among them, and the uncertainties in the data. Accurate nuclear-test data for checking fallout computations are not always available. The fallout is often poorly observed because of the great distances involved and measurement difficulties. Also, the wind field itself is poorly observed, and the variations of the wind field in time and distance are difficult to take into account in reconstructing what happened. For instance, the winds used for representing the air motion affecting the fallout for both J-S and J-U were measured just before burst from the Control Point located about 15 miles from ground zero.

It is not feasible to compare the results from the D model with those

from other models. Many important assumptions (especially concerning the initial conditions; time of start of fallout, location of the visible cloud at this time, etc.) are not clearly stated or are not stated at all in descriptions of other models. It is for this reason that comparison among the various models is virtually impossible at this time.

Pattern attributes-- The commonly-used fallout patterns indicate by means of contours of constant dose rate the dose rates (r/hr) present at 3 ft above various locations on a plane in the fallout area after fallout cessation at a reference time of 1 hr after burst (H+1 hr). The D model's ability to compute for land-surface nuclear bursts is estimated by finding how well it can describe certain obvious attributes of the fallout pattern. The pattern attributes considered in the comparisons are the following:

Axis direction
Average width
Configuration of contours around ground zero (GZ)
Magnitude of maximum dose rate
Location of maximum dose rate
Maximum downwind extent of closed contours
Areas of closed contours

Results from these comparisons are presented in the following paragraphs.

JANGLE-Surface-- Using the D model, dose rates in r/hr at H+1 hr were computed for J-S for 550 evenly-spaced locations; and the fallout pattern was constructed as shown in Figure 2. The pattern extends downwind from GZ about 4 mi, covering the area in which detailed measurements

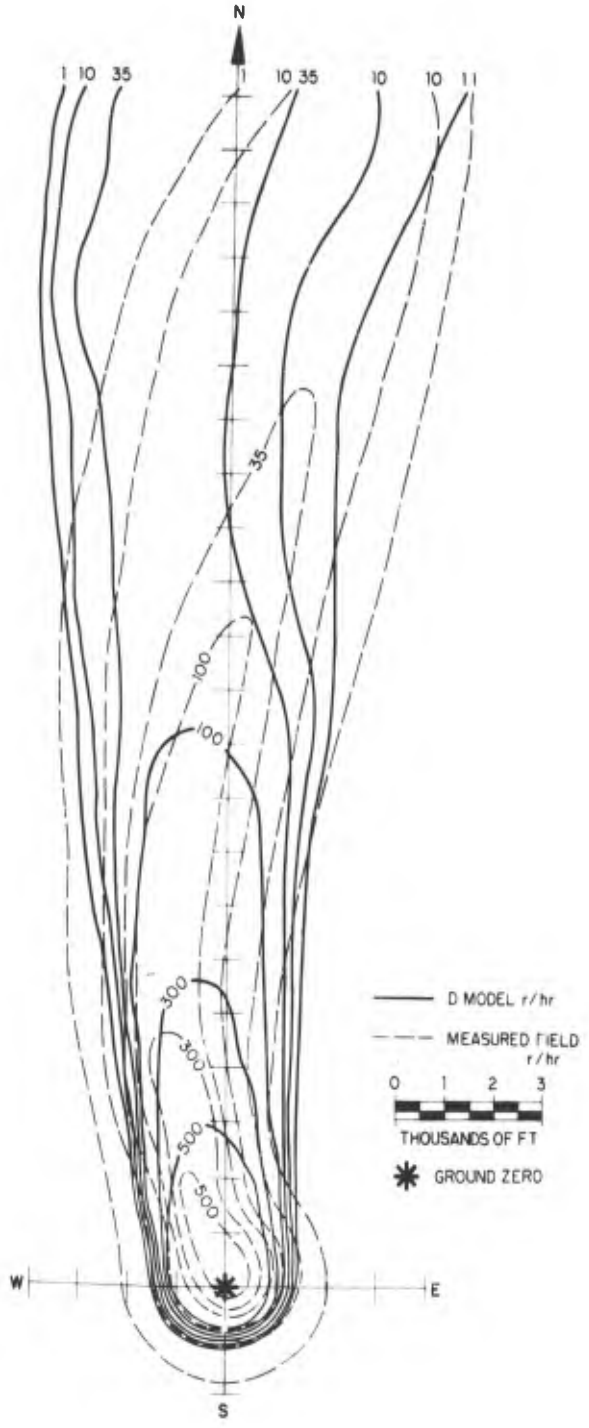

Fig. 2 D-model Dose-rate Pattern Computation for J-S at H+1 Hour

were made. The measured pattern (M pattern) shown for comparison should not be accepted as being a completely accurate representation of the dose-rate field at H+1 hr. Although it is believed to be the most accurate pattern available, it still represents the modified fallout pattern resulting from the attempt to reconcile the disagreements among three different research groups and to complete the contours for the patterns [Laurino and Poppoff]. The JANGLE dose-rate data are based primarily on readings taken with standard field ratemeters (AN/PDR-18, AN/PDR-18A, AN/PDR-18B, TIB, and CDV 710). It has been found [Work] that errors as high as 50 per cent exist in these data, even when the instruments are carefully calibrated and handled. These errors result from uncertainties due to energy dependence in the instrument, variation in instrument position with respect to the observer, and variation in orientation of instrument.

Referring to Figure 2, the overall agreement between the two patterns is very good for the axes, widths, and the configuration of the contours around GZ. In Table 2 the agreement is very good with respect to the location of the maximum dose rates, and the maximum downwind extents of the 100-r/hr, 300-r/hr, and 500-r/hr contours. The agreement is not very good for the magnitudes of the maximum dose rates and the areas enclosed by the contours. The difference between the axes at

several miles from GZ probably is due mainly to the distance variation in wind direction. The marked difference shown between the upwind extents of the 1-r/hr contours may reveal the result of ignoring the edge effect of the disks in the D model (Section 3); that is, the "shine" from the intense fallout gradient near GZ may have resulted in readings on instruments situated beyond the fallout zone. The M value for the crater is estimated to be 7500 r/hr; this is much higher than the D value of 1282 r/hr. Probably this difference occurs because the D model does not take into account any particles greater than 10,000 microns (Table 1). Since the J-S fireball was very close to the ground at start of fallout, undoubtedly heavier particles (rocks) became contaminated and fell back into the crater.

Table 2-- Comparison of M and D pattern attributes for J-S

Pattern	Maximum dose rate		Maximum contour distance from GZ (ft)			Contour area (sq mi)		
	Value (r/hr)	Distance from GZ (ft)	500 r/hr	300 r/hr	100 r/hr	500 r/hr	300 r/hr	100 r/hr
M	540	900	2200	4900	12,500	0.05	0.15	0.55
D	1450	500	3050	5800	10,500	0.21	0.43	0.96

JANGLE-Underground-- The D-model dose rates in r/hr at H+1 hr were computed for J-U for 580 evenly-spaced locations; and the fallout pattern was constructed. The D-model input data for J-U were exactly the same as J-S except for the winds. In Figure 3 the agreement between the D and M patterns is quite good for the axes, and for the configuration of the contours of value 100-r/hr and greater. Referring to Table 3, the agreement is very good for the location of the maximum dose rates and the maximum downwind extents and areas enclosed by the closed contours. The agreement is not good for the widths, configurations of contours around GZ, and the magnitudes of the maximum dose rates.

Overall, the agreement between the D and M pattern is good. With regard to the width of the M pattern, the dose-rate measurements for J-U were made after a time interval after detonation sufficiently long to allow redistribution of some of the radioactive fallout by the surface winds. The M pattern is probably broader than the D pattern around GZ because of the minor base surge for J-U (not accounted for in the D model) which surrounded GZ and extended outward several thousands of feet. Also, the M 1-r/hr contour may have been broader because of the "shine" from near GZ. An M value of 6000 r/hr is estimated for the crater's dose rate; this value (like J-S) is much higher than the D value of 1656 r/hr.

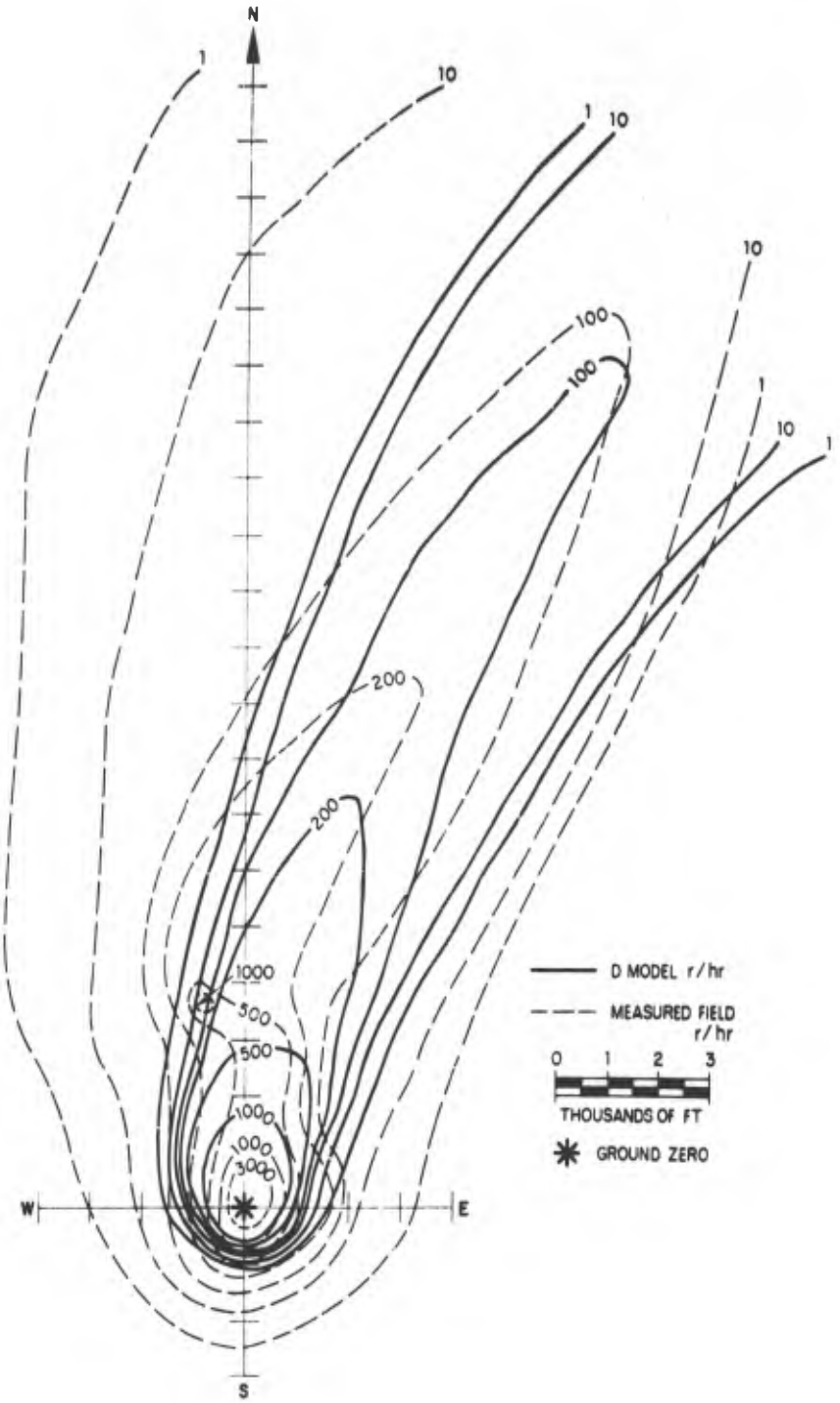

Fig. 3 D-model Dose-rate Pattern Computation for J-U at H+1 Hour

Table 3--Comparison of M and D pattern attributes for J-U

Pattern	Maximum dose rate		Maximum contour distance from GZ (ft)				Contour area (sq mi)			
	Value	Distance from GZ (ft)	1000 r/hr	500 r/hr	200 r/hr	100 r/hr	1000 r/hr	500 r/hr	200 r/hr	100 r/hr
M	3400	930	1250	3500	10,000	17,200	0.08	0.23	0.87	2.26
D	1864	500	1700	3000	7,650	16,900	0.11	0.24	0.60	1.42

A method has been developed [Anderson, 1958] to compute fallout particle-size distributions. Using this method, size-distribution computations were made with the D model [Anderson, 1959, p. 32] for J-U at ground locations 1 and 2 mi north, where size distributions were measured. Comparisons made between the computed and observed distributions showed that the D model gave consistent results; the computed distributions compared favorably with the measured distributions at both locations.

Other comparisons.-- The D-model computer program was checked further by using it to compute an H+1 hr dose rate pattern for an Operation CASTLE land-surface shot of about 100-kt yield [Anderson, 1959, p. 48]. The comparison made with locations having measured data was good. Also, the theory developed in Section 2 was used with minor modifications, by the Naval Ordnance Test Station, China Lake, California, to give a computation of the altitude profile of radioactivity at 15 min after burst for a

multi-megaton yield land-surface shot at Operation REDWING [Anderson, 1959, p. 51]. This computation showed excellent agreement with measured data.

5. CONCLUSIONS

As a result of favorable comparisons of the D-model fallout patterns with the observed test patterns for Operation JANGLE, it is concluded that the new theory is sound for fallout computation--at least for contact land-surface and shallow-underground bursts of low yield. Preliminary results indicate that the theory can be used to give successful computations for shots in the moderate-yield and high-yield ranges. The D model, derived from the theory, has been programed for a medium-size computer. Thus, it is now possible to compute for any yield and any wind condition deposit and transit dose rates and doses. Dose-rate patterns can be readily computed for any times after burst, and hence the time changes of the fallout patterns (dose-rate changes at given locations) can be taken into account. In order to compute fallout effects from high-yield bursts, it will be usually necessary to take time and distance variations of the winds into account. In principle, it is easy to do this with the computer, but in practice, it may prove difficult because of the lack of sufficient wind data. The most serious objection to this model is undoubtedly its neglect of the extreme turbulence and toroidal circulation within the rising

cloud. These subjects are difficult and do not seem thus far to have been considered by anyone. Also, it does not take into account rain scavenging. Otherwise, it is considered to approach reality in as much detail as experimental data permit.

The D model is undoubtedly the most complex model used to date for fallout computation, yet its increased intricacy has resulted in greater accuracy. It cannot at this time be considered for use in the field since its computations take many hours to make. However, this time delay does not mean that the D model has no immediate operational value. One of the main drawbacks to most fallout models has been the lack of knowledge of the size distribution vs altitude (radioactivity vs altitude) at the time the models start fallout (that is, at the time the visible cloud reaches its maximum altitude). Since the D model can be used to compute these distributions, which vary only with yield, it can help in uncovering useful simplifications necessary for operational computational techniques. Nevertheless, the main applicability of the model is to research and planning problems. Improvements in the model can be expected when additional experimental data become available.

Approved by:

W. E. Strope

W.E. STROPE, Head
Military Evaluations Division

For the Scientific Director

REFERENCES

Adams, C.E., N.H. Farlow, and W.R. Schell, The Compositions, Structures, and Origins of Radioactive Fallout Particles, U.S. Naval Radiological Defense Laboratory Technical Report USNRDL-TR-209, 1958.

Anderson, A.D., A Theory for Close-in Fallout, U.S. Naval Radiological Defense Laboratory Technical Report USNRDL-TR-249, 1958.

Anderson, A.D., Application of "Theory for Close-in Fallout" to Low-yield Land Surface and Underground Nuclear Detonations, U.S. Naval Radiological Defense Laboratory Technical Report USNRDL-TR-289, 1959.

Bolles, R.C., and N.E. Ballou, Calculated Activities and Abundances of U^{235} Fission Products, U.S. Naval Radiological Defense Laboratory Research and Development Report USNRDL-465, 1956.

Davies, C.N., Definitive Equations for the Fluid Resistance of Spheres, Proc. Phy. Soc., 57:259, 1945, London.

Government of India, Ministry of Information and Broadcasting, Nuclear Explosions and Their Effects, Chart I(a), 1958.

Laurino, R.K., and I.G. Poppoff, Contamination Patterns at Operation JANGLE, U.S. Naval Radiological Defense Laboratory Report USNRDL-399, 1953.

Minzner, R.A., K.S. Champion, and H.L. Pond, The ARDC Model Atmosphere, 1959, Air Research and Development Command Air Force Surveys in Geophysics, 115, 1959.

Special Committee on Radiation, 85th Congress, The Nature of Radioactive Fallout and Its Effects on Man, Hearings for the Joint Committee on Atomic Energy, 109, 1957.

U.S. Atomic Energy Commission, The Effects of Nuclear Weapons, 331, 1957.

Work, G.A., Evaluation of Military Radiac Equipment; Accuracy of Military Radiacs, Armed Forces Special Weapons Project AFSWP-WT-1138, 1957.

DISTRIBUTION

Copies

NAVY

1-3	Chief, Bureau of Ships (Code 335)
4-5	Chief, Bureau of Ships (Code 341)
6	Chief, Bureau of Ships (Code 423)
7-8	Chief, Bureau of Yards and Docks (D-440)
9	Chief of Naval Operations (Op-75)
10	Chief of Naval Operations (Op-07T)
11	Chief of Naval Operations (Op-03EG)
12-14	Director, Naval Research Laboratory (Code 2021)
15	CO, Naval Unit, Army Chemical Center
16	CO, Naval Air Development Center
17	Naval Medical Research Institute
18	Naval Postgraduate School, Monterey
19-20	Naval Schools Command, Treasure Island
21	CO, U.S. Naval Civil Engineering Laboratory
22	CO, U.S. Naval School (CEC Officers)
23-24	Commandant, Naval War College
25	Commander, Naval Ordnance Laboratory
26	Naval Ordnance Test Station
27	Office of Patent Counsel, San Diego
28	Commandant, U.S. Marine Corps (A03H)
29	Commandant, Marine Corps Schools, Quantico (Library)
30	Director, Marine Corps Landing Force Development Center

ARMY

31	Chief of Research and Development (Atomic Div.)
32	Chief of Research and Development (Life Science Div.)
33	Deputy Chief of Staff for Military Operations
34-36	Chief of Engineers (ENGEB)(ENGNB)(ENGWC)
37	Office of Assistant Chief of Staff, G-2
38	Ballistic Research Laboratories
39	Chief Chemical Officer
40	CG, Chemical Corps Res. and Dev. Command
41	Hq., Chemical Corps Materiel Command
42	President, Chemical Corps Board
43	CO, Chemical Corps Training Command
44	CO, Chemical Corps School (Library)
45	CO, Chemical Corps Field Requirements Agency
46-47	CO, Chemical Warfare Laboratories

48	CG, Aberdeen Proving Ground
49	Office of Chief Signal Officer (SIGRD-8B)
50	Director, Walter Reed Army Medical Center
51	Hq., Army Nuclear Medicine Research Detach., Europe
52	CG, Army Electronic Proving Ground
53	Hq., Continental Army Command (CD-CORG)
54	CG, Quartermaster Res. and Eng. Command
55	Director, Operations Research Office (Library)
56	CO, Dugway Proving Ground
57-59	The Surgeon General (MEDNE)
60	CO, Army Signal Res. and Dev. Laboratory
61	CG, Engineer Res. and Dev. Laboratory (Library)
62	CG, Engineer Res. and Dev. Laboratory (Special Projects Br.)
63	Commandant, Army Aviation School, Fort Rucker
64	President, Board No. 6, CONARC, Fort Rucker
65	Director, Office of Special Weapons Development
66	Army Map Service
67	Waterways Experiment Station
68	CO, Ordnance Materials Research Office, Watertown
69	Commandant, Command and General Staff College, Fort Leavenworth
70	Hq., Army Military District, Washington (for Booz-Allen)

AIR FORCE

71	Office of Assistant for Operations Analysis
72	Assistant Chief of Staff, Intelligence (AFCIN-3B)
73	Commander, Air Materiel Command
74-79	Commander, Wright Air Development Division (WWACT)
80	Institute of Technology, Air University (Sherwood)
81	Commander, Air Res. and Dev. Command (RDTW)
82	Commander, Air Technical Intelligence Center (AFCIN-4B1A)
83	Director, USAF Project RAND (WEAPD)
84	CG, Strategic Air Command (Operations Analysis)
85	Office of the Surgeon (SUP4), Strategic Air Command
86	Office of the Surgeon (SUP5), Strategic Air Command
87	Directorate of Engineering, Strategic Air Command
88	Office of the Surgeon General
89-90	Commander, Special Weapons Center, Kirtland AFB
91	Director, Air University Library, Maxwell AFB
92-93	Commander, Technical Training Wing, 3415th TTG
94	CG, Cambridge Research Center (CRZT)
95-96	Commander, Hq., 2D Weather Group, Langley AFB
97-100	Commander Ballistic Missile Division
101	AF Technical Applications Center

OTHER DOD ACTIVITIES

102	Chief, Defense Atomic Support Agency (Library)
103	Chief, Defense Atomic Support Agency (Radiation Div.)
104	Commander, FC/DASA, Sandia Base (FCDV)
105-114	Armed Services Technical Information Agency
115-116	National War College

OCDM

117-126 Office of Civilian and Defense Mobilization, Battle Creek

AEC ACTIVITIES AND OTHERS

127 Public Health Service (Dunning)
128 AECL, Chalk River
129 U.S. Weather Bureau, Washington (Special Projects)
130 Federal Aviation Agency
131-132 Albuquerque Operations Office
133 Argonne National Laboratory
134-136 Atomic Energy Commission, Washington
137-138 Bettis Plant
139 Brookhaven National Laboratory
140 Chicago Operations Office
141 Hanford Operations Office
142 Las Vegas Branch
143-144 Los Alamos Scientific Laboratory
145 New York Operations Office
146 Oak Ridge Operations Office
147-148 Phillips Petroleum Company
149 Public Health Service, Washington
150 San Francisco Operations Office
151 Sandia Corporation
152 Sandia Corporation, Livermore
153-155 Union Carbide Nuclear Company (ORNL)
156-170 Technical Information Service, Oak Ridge

USNRDL

171-220 USNRDL, Technical Information Division

DATE ISSUED: 22 April 1960